agronomy

MDPI

Article

Ensifer aridi LMR001^T Symbiosis and Tolerance to Stress Do Not Require the Alternative Sigma Factor RpoE2

Meryem Belfquih [1,2], Ilham Sakrouhi [1], Hassan Ait-Benhassou [1,3], Emeric Dubois [4,5], Dany Severac [4,5], Abdelkarim Filali-Maltouf [1,*] and Antoine Le Quere [1,2]

1 Laboratory of Microbiology and Molecular Biology (LMBM), Department of Biology, Faculty of Sciences, University Mohammed V in Rabat, Rabat 10100, Morocco; belfquih.meryem@gmail.com (M.B.); ilham.sakrouhi@hotmail.fr (I.S.); h.aitbenhassou@mascir.com (H.A.-B.); antoine.le-quere@ird.fr (A.L.Q.)
2 Laboratoire des Symbioses Tropicales et Méditerranéennes (LSTM), University of Montpellier, IRD, CIRAD, INRAE, Institut Agro, 34398 Montpellier, France
3 Medical Biotechnology Center, Moroccan Foundation for Advanced Science, Innovation and Research (MAScIR), Rabat Design Center, Rabat 10100, Morocco
4 Institut de Génomique Fonctionnelle (IGF), University of Montpellier, CNRS, INSERM, 34094 Montpellier, France; emeric.dubois@mgx.cnrs.fr (E.D.); dany.severac@mgx.cnrs.fr (D.S.)
5 Montpellier GenomiX, France Génomique, 34094 Montpellier, France
* Correspondence: filalimaltouf@gmail.com

Abstract: The recently proposed species *Ensifer aridi* represents an interesting model to study adaptive mechanisms explaining its maintenance under stressful pedo-climatic conditions. To get insights into functions associated with hyperosmotic stress adaptation in *E. aridi*, we first performed RNAseq profiling of cells grown under sub-lethal stresses applied by permeating (NaCl) and non-permeating (PEG8000) solutes that were compared to a transcriptome from unstressed bacteria. Then an *a priori* approach, consisting of targeted mutagenesis of the gene encoding alternative sigma factor (*rpoE2*), involved in the General Stress Response combined with phenotyping and promoter *gfp* fusion-based reporter assays of selected genes was carried out to examine the involvement of *rpoE2* in symbiosis and stress response. The majority of motility and chemotaxis genes were repressed by both stresses. Results also suggest accumulation of compatible solute trehalose under stress and other metabolisms such as inositol catabolism or the methionine cycling-generating S-adenosyl methionine appears strongly induced notably under salt stress. Interestingly, many functions regulated by salt were shown to favor competitiveness for nodulation in other rhizobia, supporting a role of stress genes for proper symbiosis' development and functioning. However, despite activation of the general stress response and identification of several genes possibly under its control, our data suggest that *rpoE2* was not essential for stress tolerance and symbiosis' development, indicating that *E. aridi* possesses alternative regulatory mechanisms to adapt and respond to stressful environments.

Keywords: *Ensifer aridi*; hyperosmotic stress response; alternative sigma factor; RNAseq

Citation: Belfquih, M.; Sakrouhi, I.; Ait-Benhassou, H.; Dubois, E.; Severac, D.; Filali-Maltouf, A.; Le Quere, A. *Ensifer aridi* LMR001^T Symbiosis and Tolerance to Stress Do Not Require the Alternative Sigma Factor RpoE2. *Agronomy* **2021**, *11*, 1787. https://doi.org/10.3390/agronomy11091787

Academic Editors: Anna Tsyganova and Viktor E. Tsyganov

Received: 20 July 2021
Accepted: 2 September 2021
Published: 7 September 2021

1. Introduction

The rhizobium strain LMR001^T (=LMG 31426^T; =HAMBI 3707^T) was isolated from desert sand dune in the Moroccan Merzouga desert [1]. This strain belongs to a new species within the *Ensifer* genus (formerly *Sinorhizobium*) that was proposed to be named *E. aridi* as isolates belonging to this new taxon were primarily isolated from arid or semi-arid environments in Africa, Asia, and America [1–3]. These bacteria are gram-negative, rod-shaped, motile, fast growing, mucous and develop a symbiotic interaction with diverse legume species able to survive under environmental constraints such as those found in deserts. More recently, *E. aridi* strains were recovered in Pakistan from mung bean grown in soils receiving as little as 12 mm of mean rainfall during the crop season [4], and strains have also been recovered from *Retama monosperma* growing in abandoned lead mine soils in

Morocco [5]. The ability to develop the symbiosis with locally growing legume species was proposed to be due to accessory genome variations among strains, which most probably result from large plasmid exchanges through horizontal gene transfer [6].

Studying nitrogen-fixing rhizobia diversity and mechanisms underlying their adaptive responses to environmental constraints such as drought or saline stresses to improve the fertility of soils and arid land resilience was raised decades ago [7]. In a context of climate change, soil degradation, and demographic growth, there is now an emergency to act and propose solutions, as warned by the latest IPCC report on Climate change and land, published in August 2019. Capable to utilize a wide range of carbon sources and to develop the symbiosis with plants adapted to environmental constraints, *Ensifer aridi* represents an interesting model to study mechanisms involved in the adaptation to aridity.

Microorganisms such as rhizobia are adapted to contrasted growth conditions (soil, rhizosphere, *in planta*) and may be recovered from contrasted pedo-eco-climatic environments. They may face oxidative, pH, acid, hyperosmotic, and/or thermal stresses during their life cycle and have developed numerous mechanisms to thrive. Among functions associated to environmental stress adaptation, bacteria use various mechanisms including cell membrane structure and composition modifications [8], tuning its permeability and transporter activity to ensure proper nutrition and ionic exchanges. For example, phospholipids and the production of surface polysaccharides may be induced to prevent water loss and maintain a hydrated microenvironment around the cell [9–11]. Bacteria may respond by a modification in the transport and/or the metabolism of several molecules such as potassium ions, sugars, or amino acid derivatives that may act as compatible solutes to counteract osmotic pressure and/or protect bacteria against intracellular damages notably in rhizobia [12]. Among them, trehalose, a non-reducing disaccharide, appears promising as it may improve plant stress tolerance through symbiosis-mediated accumulation [13]. Bacteria may also trigger repair mechanisms to protect their macromolecules against damages by reactive oxygen species [14]. Finally, several transcription factors are also involved to modulate gene expression and enable the bacteria to rapidly respond to environmental changes through specific regulatory pathways.

Indeed, when subjected to environmental stressors, alphaproteobacteria, the bacterial class to which rhizobia belong, induce a conserved General Stress Response (GSR) that involves a regulatory system composed of an Extra Cytoplasmic Function (ECF) sigma factor (σ^{ECFG}), an anti-sigma factor (NepR), and an anti-anti sigma factor (PhyR), whose activity depends on its phosphorylation by the Histidine kinase PhyK [15]. More recently, Lori and colleagues showed the involvement of a single domain response regulator MrrA as an intermediate between histidine kinases and PhyK, suggesting that PhyK may act as a phosphotransferase rather than a phosphate kinase [16]. Inducing molecules interacting with the primary sensors and some regulatory proteins involved in the GSR regulation remain to be determined. However, the phosphorylation of the multi-domain alternative two component system protein PhyR leads to its binding to the anti-sigma factor NepR, which is under normal growth conditions bound to σ^{ECFG}, thus releasing its interaction with RNA polymerase, which triggers GSR [15].

Here, to explore the regulatory response of the new species *E. aridi* to salt- or water-induced hyperosmotic stresses, a genome-wide transcriptional study was performed. A mutant in the *Ensifer aridi* LMR001 σ^{ECFG} encoding gene (*rpoE2*) was generated and studied to evaluate its involvement in the GSR-mediated regulation of salt-induced osmotic upshift of selected metabolisms' transport and regulation or to assess the importance of the GSR to cope with such stress and to develop the symbiosis with compatible hosts.

2. Materials and Methods

2.1. Bacterial Growth

The bacterial strains and plasmids used in this study are listed in Table 1. *Ensifer* strains and derivatives were cultured in tryptone yeast extract (TY) medium [17] at 28 °C. *Ensifer* cultures were routinely started from glycerol stocks upon a primary growth on

TY agar plates. *E. coli* strains were grown at 37 °C in Luria-Bertani medium [18]. Solid media contained 2% agar. Gentamycin (Gm, 10 μg mL^{-1}), kanamycin (Km, 50 μg mL^{-1}), ampicillin (Ap, 50 μg mL^{-1}), rifampicin (Rif, 100 μg mL^{-1}), and 5-bromo-4-chloro-3-indolyl-beta-D-galactosidase (X-gal, 80 μg mL^{-1}) were added to the media for selection as required.

2.2. Phenotypic Characterization of the ΔrpoE2 Strain

2.2.1. Plant Nodulation Assay

Seeds of *Vachellia tortilis* subsp. *raddiana* and of the endemic Moroccan *Vachellia gummifera* [19] were scarified and surface sterilized in concentrated sulfuric acid (95%) with agitation for 1 h for *V. tortilis* and 30 min for *V. gummifera* and rinsed thoroughly with sterile water. Seeds were then germinated on water agar plates at 25 °C for 5 days in the dark. After germination, seedlings were planted in pots containing sand that was previously sterilized by autoclaving for 1 h at 120 °C. *Ensifer aridi* LMR001 WT and Δ*rpoE2* were pre-grown in TY medium up to an optical density (OD) 600 nm of 0.7 and then washed and re-suspended in sterilized water prior to inoculation using 1 mL of washed cells directly after planting. Six individual plants were inoculated with each rhizobial strain or sterile water for the negative and positive controls. Plants were incubated in a growth chamber at 26 °C under a photoperiod of 16 h day and 8 h night and watered using N-free plant growth BD medium for watering [20] that was supplemented with KNO_3 (3 mM) as a source of nitrogen for the positive controls. After 6 months of growth, the plants were harvested, and nodule number, plant shoot, and root fresh weights were recorded.

2.2.2. Motility Assay

LMR001 and Δ*rpoE2* were grown at 28 °C in TY broth with shaking at 180 RPM to an OD (600 nm) of 0.7. After incubation, cells were pelleted, washed twice with sterile water, and resuspended in 10 volumes of sterile water. Swimming test assays were performed using 20 mL of TY media that were complemented either with 0, 5.85, or 11.7 $g{\cdot}L^{-1}$ NaCl (generating, respectively, ≈0, 0.1, and 0.25 M final NaCl concentrations) and 0.2% agar. Each medium was poured into Petri dishes, upon cooling to 50 °C in a water bath to avoid water loss by evaporation, and allowed to solidify in a horizontal laminar flow for 15 min. Finally, aliquots (5 μL) of washed cells were gently dispensed into the center of the plates and incubated at 28 °C for 5 days and the diameters of motile bacteria were measured after 2, 3, and 5 days of growth. The average diameter and the standard deviations from three biological replicates were calculated.

2.2.3. Salinity Tolerance

Ensifer aridi LMR001 and Δ*rpoE2* derivatives were first grown in liquid TY cultures up to an OD (600 nm) of 0.7, and 1 mL was used to inoculate 50 mL of liquid TY medium as well as TY complemented with 14.6, 17.5, or 23.4 g L^{-1} of NaCl (generating, respectively, 0.25 M, 0.3 M, and 0.4 M final salt concentrations). Cultures were incubated in a rotary shaker (180 RPM) at 28 °C and the OD (600 nm) was recorded after 4, 8, 24, 48, 120, and 144 h incubation. The mean ODs (600 nm) of three independent cultures were calculated for both strains and at each time point with their respective standard deviations.

2.2.4. Sensitivity to Detergent, Acid, and Oxidative Stresses

Sensitivities to oxidative, acid, and detergent stresses induced, respectively, by H_2O_2, HCl, and SDS were compared between the wild-type LMR001 and the Δ*rpoE2* strains. Briefly, 4 mL of bacterial cultures of *E. aridi* or the Δ*rpoE2* strain (pre-grown to OD 600 nm ≈ 0.7 in TY liquid medium) were added to 16 mL of soft TY agar containing 0.7% of agar precooled to 45 °C and poured onto TY agar plates. Once solidified, a paper disc (6-mm diameter) was placed on the plate and 5 μL of H_2O_2 (2 M), HCl (5.5 M), or SDS (10% *w*/*v*) was spotted onto it. Plates were incubated at 28 °C for three days prior

to recording the diameters of the inhibition zones, and the average of three replicates were averaged.

2.3. RNAseq Analysis and Characterization of Differentially Regulated Genes in LMR001 upon NaCl- or PEG8000-Induced Hyperosmotic Stresses

For the RNAseq analysis, the method was adapted from previously published work [21]. Briefly, six biological replicates were first grown in TY medium up to an OD (600 nm) of 0.9 (±0.05) in 250 mL Erlenmeyer flasks at 30 °C with 140 rpm. For each replicate, 15 mL were added to an equal volume of pre-warmed TY containing either nothing (Controls), NaCl at 500 mM (Salt treatment, 250 mM final concentration), or PEG8000 at 24% (W:V) (PEG8000 treatment, 12% final concentration), and were further incubated at 30 °C and 140 rpm. After 2 $\frac{1}{2}$ h of incubation, which is less than a generation time, 1/10th volume of stop buffer (ethanol containing phenol at a final concentration of 5%) was added to each culture (6 replicates × 3 treatments) to inhibit RNAses and centrifuged 4 min at 8000× *g* and 4 °C. The pellets were snap-frozen in liquid nitrogen and kept in the freezer at −80 °C until use.

Total RNAs were purified from each replicate and treated with the RiboPure™ kit (AMBION), which included a DNAse I treatment, according to manufacturer's recommendations. RNA extracts from the six replicates were then pooled and subjected to two successive rounds of rRNA subtractions with Microbe Express™ kit (AMBION), following manufacturer's recommendations. Purified mRNAs were sent to Montpellier Genomix for sequencing. Three libraries corresponding to the three treatments (Control, Salt, and PEG8000) were prepared, following illumina kit instructions. Briefly, for each library, 100 ng of mRNA were first fragmented chemically, and reverse transcribed using random primers and SuperScript II™ to generate first-strand cDNAs. The second strand was synthesized using DNA polymerase I and RNAse H. The cDNA fragments were then end-repaired, a single 'A' base was added, and adapters were ligated. These products were enriched by PCR to select for cDNA fragments containing adaptors and to create the final cDNA library. The efficacy of the library construction was checked in a quality control step that involved measuring the adapter-cDNA size and concentration on an Agilent DNA 1000 chip. Sequencing libraries were denatured with sodium hydroxide and diluted to 6 pM in hybridization buffer for loading onto a single lane of an Illumina HiSeq 2000 flow-cell V1.5. Cluster formation, primer hybridization, and single-read, 100 sequencing cycles were performed on cBot and HiSeq2000 (Illumina, San Diego, CA, USA), respectively.

After sequencing, reads that passed the sequencing platform quality filter were imported into CLC Genomics workbench (V5.5.1) and mapped to the RAST-predicted genomic objects [6] including putative protein encoding genes (PEGs) (listed in Table S1) and RNAs from *Ensifer aridi* LMR001 using 95% of sequence similarity over 70% of read length. Reads that mapped several PEGs were discarded. Finally, the read table obtained upon mapping the three libraries onto PEGs were normalized using a LOESS transformation that appeared to be the most adapted method, as the PEG8000 treatment resulted in an enhanced recovery of the least abundant transcripts as compared to the control or salt treatments (see Section 3). Genes showing an average coverage of 50× and more than 2-fold differences between pairwise comparisons were considered as differentially regulated.

To explore the major changes associated to the transcriptomes, the predicted proteome of the LMR001 strain was functionally annotated using COG and KEGG classifications [22,23]. Differentially regulated genes were then used to estimate major classes and functions associated to salt- and PEG8000-induced hyperosmotic stresses.

2.4. Real-Time PCR on Selected Genes

The list of genes targeted, as well as primers used for real-time PCR experiments, are listed in Table 1. LMR001 was cultivated either in TY or in TY complemented with NaCl at 250 mM, as described for the RNAseq experiment. Three biological replicates for each growth condition were extracted using SV Total RNA Isolation kit (Promega), following manufacturer's recommendations. RNA samples were treated with Turbo DNAse (Applied

Biosystems) to remove any DNA contaminant from RNA samples. For each sample and replicate, 1 µg of total RNA was reverse-transcribed with 400 U of Super-Script II (Invitrogen) and random hexamer primers. The qPCRs were performed on a Strategene MXP3005P system using Power SYBER green master mix (Applied Biosystems). PCR cycling conditions consisted of a primary 10-min incubation at 95 °C, followed by 40 cycles consisting of 15 s at 95 °C and 30 s at 60 °C. Primer specificity and efficiencies and the formation of primer dimers were estimated by dissociation curves. The expression levels of a selection of 12 genes were standardized by using the gene *hrcA* as reference. PCR efficiency (E) for each amplicon was calculated using the linear regression method on the log (fluorescence)-per-cycle-number data using Stratagene MXpro software. All qPCRs were performed in two technical replicates using total RNA isolated from three biological samples so as to assess biological variability. Data for each sample were expressed relative to the expression levels of *hrcA* by using the mathematical model described previously, which determines the relative quantification of a target gene in comparison to a reference (ref) gene between treatment and control samples [24]. The relative expression ratio (R) of a target gene is calculated based on efficiency (E) and the threshold cycle (Ct) of an unknown sample versus a control and expression in comparison to a reference gene. The average relative quantity for each gene under study was calculated and log2-transformed. Means and standard deviations of these final log2 ratios were calculated using data from three biological replicates.

2.5. LMR001 ΔrpoE2 Mutant Construction

The regions bordering the *rpoE2* gene (PEG2539) were first amplified by PCR with custom-designed primers (see Table 1). The primer pair rpoE2-P2539-A-XI/rpoE2-P2539-B-HIII was used to amplify a 478 bp sequence located upstream of the *rpoE2* gene including the first 37 bases of the coding sequence. Furthermore, the primer rpoE2-P2539-B-HIII contained in 5′ a HindIII site as well as 13 bases that were complementary to the 5‘ end of the primer rpoE2-P2539-C-HIII that was used together with rpoE2-P2539-D-XI to amplify a 473 sequence of the 3′ region of the *rpoE2* gene including the last 77 nucleotides. The PCR was performed using, as templates, genomic DNA extracts from LMR001 obtained, following the method reported previously [25], using 10 mL of bacterial liquid cultures at early stationary phase. First, PCR reactions were performed to amplify both the 5′ and the 3′ flanking regions using the proof-reading enzyme Phusion (Thermo-Fischer) and recommended chemistry, except for primers (1 µM final concentrations for forward and reverse primers). The cycling conditions included a primary denaturation step of 30 s at 98 °C followed by 35 cycles (98 °C, 10 s/56 °C, 30 s/72 °C, 45 s) and a final elongation step of 7 min at 72 °C. PCR products were purified using Illustra™ GFX PCR DNA and Gel Band purification kits (GE Healthcare), following manufacturer's recommendations. Then a second PCR reaction was set up, using as primers and matrix, purified PCR products obtained that contain complementary sequences, thus enabling priming of the amplification. The 25-µL reactions contained 5 µL of 5× GoTaq buffer (Promega), 1.25 µL of $MgCl_2$ (25 mM), 2.5 µL of dNTP mix (2.5 mM each), 0.125 µL GoTaq (5 U/µL), 2 µL of each purified PCR products obtained, and nuclease free water. A primary PCR cycling consisting of a denaturation step of 95 °C for 5 min followed by 5 cycles (95 °C, 30 s/50 °C, 45 s/72 °C, 50 s) and 5 min at 72 °C was performed so as to generate chimeric DNA molecules consisting of merged 5′ and 3′ regions. Then, 15 µL of the mix (3 µL of 5× GoTaq buffer, 0.75 µL of $MgCl_2$ (25 mM), 1.5 µL of dNTP mix, 0.125 µL of GoTaq (5 U/µL), 4 µL of external primers rpoE2-P2539-A-XI and rpoE2-P2539-D-XI, and 1.625 µL of nuclease free water) was added to the PCR reaction and subjected to the following cycling conditions: a denaturation step of 95 °C for 5 min followed by 25 cycles (95 °C, 30 s/55 °C, 45 s/72 °C, 50 s) and 5 min at 72 °C. The PCR product was purified from 1% agar gel using promega Wizard®® SV Gel and PCR Clean-Up System, following recommended protocol. As a result of the two amplifications' process, the PCR-amplified and -purified product was cloned as a fragment into a pGEM-T Easy Vector (Promega kit) and transferred into XL2-Blue

Ultra-competent Cells. The resulting positive clones were selected and the plasmid was extracted by using the Wizard®® Plus SV Minipreps DNA Purification System, digested by XbaI enzyme and ligated into suicide vector pJQ200SK [26]. Enzymes were purchased from Promega. The latter plasmid was used to transform *Ensifer aridi* LMR001 cells by bipartite conjugation method using S17-1 *E. coli* strains as a donor [27]. Transformants were selected on TY plates containing Rif and 5% sucrose to allow selection of knockout clones that had undergone a double cross-over. Double cross-over gene replacement in mutants was verified by screening for antibiotic resistant/ sensibility phenotypes (Rif and Gm, respectively) and also PCR to verify deletion by using specific external and internal primers.

Table 1. Strains, plasmids, and primers used in the study.

Strains Plasmids Primers	Description/Primer Sequence	Source/Reference
Strains		
***Escherichia coli* strains**		
XL2 Blue Ultra-competent Cells	*endA1 supE44 thi-1 hsdR17 recA1 gyrA96 relA1 lac* [F′ proAB *lacIqZ*ΔM15 Tn10 (Tetr) Amy Camr]	Stratagene
S17-1	*recA* [SmR], thi, pro, *RP4*-2-Tc:Mu: *aph*::Tn7λpir.	[27]
***Ensifer aridi* strains**		
LMR001^T	*Ensifer aridi* LMR001^T (=LMG 31426^T; =HAMBI 3707^T)	[1,2]
LMR001 Δ*rpoE2*	*rpoE2* deletion mutant of *Ensifer aridi* LMR001^T	This work
Plasmids		
pGEM-T Easy	Amp^R, pUC origin, Multi Cloning Sites), *lacZ* gene fusion, β-lactamase coding region, *lac* operon sequences.	Promega
TOPO vector	Km^R, Amp^R, pUC origin, *lacZ α-ccdB* gene fusion. Topoisomerase enzyme	Invitrogen
pPROBE NT (pNT)	Km^R, pBBR1 replicon, Multi Cloning Sites upstream of *gfp* reporter gene	[28]
pJQ200SK+	Gm^R, SacB; Ori origin replication, mob region, Multi Cloning Sites	[26]
pNT-*sahR*p	pPROBE NT containing *sahR* (PEG2239) promoter fused to *gfp* gene, KmR	This work
pNT-*nesR*p	pPROBE NT containing *nesR* (PEG5735) promoter fused to *gfp* gene, KmR	This work
pNT-*rsiA1*p	pPROBE NT containing *rsiA1* (PEG2540) promoter fused to *gfp* gene, KmR	This work
pNT-*rsiB1*p	pPROBE NT containing *rsiB1* (PEG2541) promoter fused to *gfp* gene, KmR	This work
pNT-*thuE*p	pPROBE NT containing *thuE* (PEG6268) promoter fused to *gfp* gene, KmR	This work
pNT-*otsB*p	pPROBE NT containing *otsB* (PEG4868) promoter fused to *gfp* gene, KmR	This work
pNT-*treZ*p	pPROBE NT containing *treZ* (PEG5323) promoter fused to *gfp* gene, KmR	This work
pNT-PEG4866p	pPROBE NT containing a glycosyl transferase encoding gene (PEG4866) promoter fused to *gfp* gene, KmR	This work
pNT-*thuR*p	pPROBE NT containing *thuR* (PEG6269) promoter fused to *gfp* gene, KmR	This work
pNT-*iolC*p	pPROBE NT containing *iolC* (PEG373) promoter fused to *gfp* gene, KmR	This work
pNT-*iolR*p	pPROBE NT containing *iolR* (PEG374) promoter fused to *gfp* gene, KmR	This work
Primers		
Targeted gene primers for qPCR		
iolB (PEG370) Forward	5′-CGGGCACACGTCCTCCTATC-3′	This work
iolB (PEG370) Reverse	5′-CCCTTGGGTACCAGCGTGAC-3′	This work
flgB (PEG666) Forward	5′-CCCAGGTGACCGAGGTGAGT-3′	This work
flgB (PEG666) Reverse	5′-CCCCGCATTGAGCTCGTAGT-3′	This work
hrcA (PEG397) Forward	5′-ACCAAGGGGATCGCATCGAC-3′	This work
hrcA (PEG397) Reverse	5′-GGCTCGCCGCTTTCCAGATA-3′	This work
metK (PEG438) Forward	5′-CCCAGCCGCTGTCGATCTAT-3′	This work
metK (PEG438) Reverse	5′-GGCGAGAGGTCCATCGTCTT-3′	This work
cheA (PEG646) Forward	5′-TCCGCTCCGTTTTCGAGTTC-3′	This work
cheA (PEG646) Reverse	5′-GCAACGGTCCGATCCTCTTC-3′	This work
gltA (PEG1564) Forward	5′-ATTGCGCTGACGGACGAGTAC-3′	This work
gltA (PEG1564) Reverse	5′-GCGTGATGCCGGAATAGAAG-3′	This work
ahcY (PEG3556) Forward	5′-AAGGGCAACCGCATCATTC-3′	This work
ahcY (PEG3556) Reverse	5′-GCTTCGGCAGCACGTAGAC-3′	This work

Table 1. *Cont.*

Strains Plasmids Primers	Description/Primer Sequence	Source/Reference
Primers		
Targeted gene primers for qPCR		
metH (PEG3206) Forward	5′-TGGGAGCTGAAGGGCGTCTA-3′	This work
metH (PEG3206) Reverse	5′-TCGGTGAAAAGGCGGATGTC-3′	This work
bhMT (PEG1969) Forward	5′-GCGGGTCCGAGATCCACTATT-3′	This work
bhMT (PEG1969) Reverse	5′-CGCAGCAGCCTCCGATGAT-3′	This work
sahR (PEG2239) Forward	5′-ATTTCCGCCTGCGTCAAGAG-3′	This work
sahR (PEG2239) Reverse	5′-CGGCGTTGCGACTGAAATAG-3′	This work
L11MT (PEG2189) Forward	5′-ACAAGGTGAAGGCGGGTGAG-3′	This work
L11MT (PEG2189) Reverse	5′-GAGGTCGAGGACGTTGCAGAA-3′	This work
xylF (PEG2505) Forward	5′-GCTCGGCACCCAGACTGTTT-3′	This work
xylF (PEG2505) Reverse	5′-GGTCTGCACGCCTTCGATCT-3′	This work
thuE (PEG6268) Forward	5′-GCTCCGGCGCTCTACTATCG-3′	This work
thuE (PEG6268) Reverse	5′-GGCGTTTGCCTGGAAGACA-3′	This work
Primers for *rpoE2* deletion mutant construction		
RPOE2-P2539-A-XI	5′-CCTCTAGACATCGCCTGAGGTCTGAGAT-3′	This work
RPOE2-P2539-B-HIII	5′-CGCCCTTCACTTGAAGCTTGCATCTCACGCTTGAACTCT-3′	This work
RPOE2-P2539-C-HIII	5′-AAGCTTCAAGTGAAGGGCGAGAAC-3′	This work
RPOE2-P2539-D-XI	5′-CCTCTAGATTGACCCATTGCCATTCACG-3′	This work
Targeted gene promoter/Primers for promoter::*gfp* fusion cloning		
*iolR*p Forward/iolR-1	5′-GACTTCCGCGAGGGCTAC-3′	This work
*iolR*p Reverse/iolR-B	5′-TCGGCCTCGACGGAGGGACATCGGTGGTCG-3′	This work
*iolC*p Forward/iolC-1	5′-CTCGCTTTCGGCAAGC-3′	This work
*iolC*p Reverse/iolC-B	5′-GGCGACGGCTTGGCCGATCGTGATGATGTC-3′	This work
*sahR*p Forward/metReg-1	5′-CAATCCGAAGCGGGTG-3′	This work
*sahR*p Reverse/metReg-B	5′-GTTTTCCTTCCTGGCGTTCCTCTGTCACCC-3′	This work
*nesR*p Forward/nesR-1	5′-GGTTTCCGGGCCTGCAC-3′	This work
*nesR*p Reverse/nesR-B	5′-TTAAGCCGCGGCGGTGAACTGGTTCCTGATC-3′	This work
*rsiA1*p Forward/rsiA1-1	5′-GAAGGTAAGGAAGGAATG-3′	This work
*rsiA1*p Reverse/rsiA1-B	5′-GAATCGATTGTCCCGCAATCTGTACATTCG-3′	This work
*risB1*p Forward/rsiA1-B	5′-GAATCGATTGTCCCGCAATCTGTACATTCG-3′	This work
*risB1*p Reverse/rsiA1-1	5′-GAAGGTAAGGAAGGAATG-3′	This work
*otsB*p Forward/peg4866-B	5′-AGCTTATCGAGAGCAATTTGCGCGATCTTC-3′	This work
*otsB*p Reverse/peg4866-1	5′-CTCGATCATGGAGAGG-3′	This work
PEG4866p Forward/peg4866-1	5′-CTCGATCATGGAGAGG-3′	This work
PEG4866p Reverse/peg4866-B	5′-AGCTTATCGAGAGCAATTTGCGCGATCTTC-3′	This work
*treZ*p Forward/treZ-1	5′-GAGCTCGGGTTTGATG-3′	This work
*treZ*p Reverse/treZ-B	5′-CGAAAGGTTGACCGTCGCTGTCTCTCGCAT-3′	This work
*thuR*p Forward/thuR-1	5′-CTCGAAGGCTCCTCAGC-3′	This work
*thuR*p Reverse/thuR-B	5′-AGCAATTGCAGCGCGAACTCCTTGAGCTTC-3′	This work
*thuE*p Forward/thuR-B	5′-AGCAATTGCAGCGCGAACTCCTTGAGCTTC-3′	This work
*thuE*p Reverse/thuR-1	5′-CTCGAAGGCTCCTCAGC-3′	This work
gfp Reverse/gfp-Rev50	5′-ACATCACCATCTAATTCAAC-3′	This work

2.6. Use of Promoter-Gfp Fusions for Transcriptional Analyses in the Wild-Type and the ΔrpoE2 Strains

The promoter region of genes involved in the regulation of the methionine cycle (*nesR*, PEG5735; *sahR*, PEG2239), in the regulation of the GSR (*rsiA1*, PEG2540; *rsiB1*, PEG2541), in the trehalose transport (*thuE*,PEG6268) metabolism (*otsB*, PEG4868; *treZ*, PEG5323), a glycosyl transferase (PEG4866) located upstream of the *otsBA* operon in reverse orientation or the regulation of trehalose transport and endogenous utilization (*thuR*, PEG6269), and in the inositol catabolism (*iolC*, PEG373) and regulation (*iolR*, PEG374) was amplified using

primers listed in Table 1. PCR products were cleaned up using illustra™ GFX™ PCR DNA and Gel Band Purification Kits (GE Healthcare). The purified PCR products were ligated into TOPO®® TA Cloning®® vector (INVITROGEN), following the manufacturer's recommendations, and were transferred into *E. coli* XL2 Blue Ultra-competent Cells. Plasmid DNA was extracted using the Wizard Plus SV Minipreps DNA Purification System kit (Promega), following the manufacturer's recommendations. Plasmids containing the promoters were sequenced by Genoscreen (Lille, France) to verify sequence integrity. Inserts were excised using the restriction enzyme EcoRI and ligated into a pPROBE NT vector, which allows for transcriptional fusions with the green fluorescent protein (GFP) encoding gene *gfp* [28], previously digested with EcoRI and dephosphorylated. The ligation mix was transferred into electro-competent *E. coli* strain S17-1. The selection of clones containing the promoters in the proper orientation was done by using the forward primers of the promoters with the primer gfp-Rev50 located in the reverse orientation of the 5′ end of the *gfp* gene, which results in positive PCR amplification when correct. The pPROBE NT constructs were transferred into LMR001 Rif^R or Δ*rpoE2* strains by biparental mating. Briefly, Donor S17-1 cells containing the pPROBE NT derivatives were grown on LB agar containing Kanamycine (50 μg mL^{-1}) and the recipient cells were grown onto TY Agar containing Rifampicine (100 μg mL^{-1}). Half a loop of donor cells and 2–3 loops of recipient cells were resuspended in separate Eppendorf tubes containing 1 mL of TY medium each to wash cells from antibiotics. The tubes were mixed by mild vortexing and centrifuged at 7000× *g* for 7 min and resuspended in 0.5 mL of fresh TY medium. Then, 100 μL of each of the donor and the recipient cells were mixed onto fresh TY plates and grown for 2 days at 28 °C. Half loops of cells were then streaked onto a TY agar plate containing the two antibiotics (Kanamycine and Rifampicine) for selection of transconjugants. Individual colonies were finally isolated and verified by PCR prior conservation in 20% glycerol at −80 °C. When needed, strains carrying the promoter pPROBE constructs were grown on TY agar plates supplemented with appropriate antibiotics at 28 °C. Using sterile toothpicks, fresh colonies were transferred to 10 mL liquid TY containing Kanamycine and grown overnight with shaking at 28 °C. Cells were washed in fresh TY medium and resuspended in an equal volume of fresh TY medium prior to use in transcriptional assays. For each transcriptional assay, the same bacterial inocula (70 μL) were used to inoculate 140 μL TY medium supplemented or not with NaCl (250 mM final concentration) in 96-well plates. The plates were transferred in a spectrofluorometer microplate reader (TECAN Infinite M200) set at 28 °C and subjected to the following cycling conditions. After a preliminary shaking of 900 s using orbital shaking mode with 1-mm amplitude, the mean of three reads of optical density (600 nm) and three reads of fluorescence levels (excitation filter at 485 nm and emission filter at 535 nm) were recorded every 30 min for all wells and at least 9 h. The experiment was performed three times. For the analysis, each plate was treated separately and relative fluorescence values were recorded as follow. First, the fluorescence data were transformed for each time point as a percentage of the maximal fluorescence levels observed in the experiment to enable the comparison between each replicate. The relative fluorescence values were finally obtained by dividing the normalized fluorescence obtained by the corrected OD600 nm measures at each time point. Data from the bacterium containing empty vector were finally subtracted and the means from the three independent repetitions were finally calculated.

3. Results and Discussion

To explore the possible mechanisms that *Ensifer aridi* possibly uses to face hyperosmotic stresses, a transcriptomic approach was realized using NaCl as a permeating solute and PEG8000 as a non-permeating solute that, respectively, resulted in salt- and water-induced osmotic upshifts. To focus on functions associated with these stresses and disregard mechanisms linked to cell death, mild stresses were triggered using sublethal concentrations for less than a generation time. First, growth kinetics of LMR001 were compared in TY medium containing various concentrations of Salt (NaCl) and PEG8000.

Concentration of 250 mM of salt and 12% (w/v) of PEG8000 were chosen, as these concentrations reduced the growth of the bacterium without inhibiting its growth. Indeed, six independent cultures were pre-grown in TY Medium up to an OD (600 nm) of 0.9. Each pre-culture was further used to inoculate an equal volume of either TY or TY complemented with Salt 0.5 M (0.25 M final concentration) or with PEG8000 24% w/v (12% final concentration). After 2 $\frac{1}{2}$ h of incubation, the mean OD (600 nm) of the control rose from 0.52 to 0.94 (ΔOD = 0.42), which was significantly higher than the ΔOD obtained in media containing salt and PEG8000 (-10% in PEG8000 growth medium and -40% in salt containing medium; p-values < 0.05, Student Test), confirming that bacteria were subjected to a mild stress that did not inhibit totally their growth.

All cultures were subjected to a total RNA extraction and purified RNAs were pooled according to the treatments prior to rRNA subtractions. Finally, enriched mRNA samples from controls (TY), salt-stressed bacteria (250 mM NaCl), or Water-stressed bacteria (12% PEG8000) were sent for sequencing at the Montpellier MGX sequencing platform. Sequencing consisted of 100 cycles on Hiseq2000 that generated, respectively, 109.95-, 95.17-, and 105.89-million sequence reads of 100 bp (>31 Gb). For each library, the reads were mapped to the LMR001 RAST Predicted Encoding Genes (PEGs) and rRNAs as well as the spike phiX using CLC genomics Workbench (see Materials and Methods for parameters used). Results of the sequencing and mapping are shown in Figure S1. Even though the number of reads that mapped to rRNAs were high (55.39, 35.1, and 39.23 million reads for control, salt, and PEG libraries, respectively), the procedure enabled us to recover significant numbers of reads that mapped to LMR001-predicted encoding gene sequences (respectively 34.91, 35.12, and 42.79 million reads). If we consider that 95% of the RNAs in cells are corresponding to ribosomal RNAs, while only 5% are mRNAs, the rRNA subtraction procedure enabled the removal of 91.6%, 94.7%, and 95.2% of rRNAs (respectively, for the libraries TY, TY + 250 mM salt, and TY + 12% PEG8000). These rates are comparable to those obtained in *Mesorhizobium* [21] and indicate that the procedure is also well suited to *Ensifer aridi*.

Scatter plots showing distributions of reads obtained upon mapping on LMR001 PEGs in control (X Axis) as a function of salt or PEG8000 treatments (Y Axes) (Figure S2A,B, respectively) or M-A plots (showing the logarithmic values of mean read numbers for control and salt or control and PEG8000, as a function of the log2 ratios (Figure S2C,D, respectively)) indicated that while salt and control showed rather centered distributions, the sample PEG8000 returned a strong bias for lowly expressed transcripts that were over-represented in this library as compared with control and salt libraries. This bias may result from the presence of PEG8000 remaining in pelleted cells as these molecules favor precipitation of nucleic acids [29,30]. To estimate whether the presence of PEG8000 in the samples also influenced the recovery of particular size fractions of the RNAs, we compared the relative abundances of read counts in the three libraries upon normalization to the total read numbers mapped to PEGs for all predicted genes and ordering based on PEG size, their mean sequencing coverage (obtained from the three libraries), and, finally, by predicted gene order, which is independent of size or coverage. Figure S3 shows the relative abundances of reads obtained in the three libraries (Y axis) for all genes upon ordering, as described above (X axes), as a piled 100% Surface area graphics. The comparison of profiles confirmed that only a bias toward predicted genes lowly transcribed was found. These results clearly show that the PEG8000 facilitated the recovery of rare transcripts using the method used here, and that this enrichment was higher as the coverage was lowering (Figure S3B).

Furthermore, box plots showing the distributions of raw read counts (as log values) in the three libraries also indicated differences in sequencing medians and quartile values (Figure S2E). To normalize for differences in sequencing depth between the three libraries and obtain statistics on differentially regulated genes without multiple replicates, DESeq can be used [31]. However, given the strong bias obtained from the PEG8000 library that generates incomparable expression levels for the genes that are the least transcribed, we could not use this package, and lack statistics from the RNAseq data. In order to

normalize for the bias related to lowly expressed genes' enrichment in the PEG8000 library and for the sequencing depth differences in the three libraries, we performed locally estimated scatter plot smoothing (LOESS) using a window of 0.1 (Log read counts) for both comparisons, Control vs. Salt or PEG8000. This normalization step enabled us to retrieve expected read counts from all three libraries and to obtain the relative abundances of each gene in the three libraries. As expected, distributions of normalized data presented more centered distributions (Figures S2F–J and S3D–F) even though a slight bias for the least transcribed genes remained visible for genes whose coverage was below 30× mean coverage (Figure S3E). To support the RNAseq data, a selection of genes was analyzed by RT-qPCR using fresh bacterial cultures.

The relative expression of 12 genes showing contrasting expressions levels upon salt stress was monitored using *hcrA* as normalizer by qPCR assays on samples obtained from three independent samples. This analysis indicated a good correlation with RNAseq data (R2 = 0.917) (Figure S4), which confirms that RNAseq data can be used to explore the major changes associated with stress under study, even though qPCR data indicated lower differential expressions as compared to RNAseq, the latter representing a direct measure of transcript levels.

To explore functions associated to salt- and water-induced hyperosmotic stresses, predicted genes showing 50× of mean coverage between two compared treatments (Salt vs. Control or PEG8000 vs. Control) and presenting fold changes of 2 or greater were first selected. Analyses of COGs and KEGG orthologous assignation of differentially regulated genes enabled us to estimate major metabolic and cellular functional changes associated to stresses. Table S1 shows the entire list of LMR001-predicted encoding genes (PEGs), their predicted annotations (RAST-SEED based, COG classification, and KEGG orthology), and RNAseq data.

Globally, we found that salt stress induced a stronger transcriptional response as compared to PEG8000. Addition of salt in the medium triggered an induction of 473 PEGs and a repression of 708 PEGs, of which 331 and 549, respectively, were classified into at least one COG class. In the PEG8000 treatment, only 75 PEGs presented more than 50× mean coverage and a 2-fold induction, and 237 were repressed, of which, 67 and 122, respectively, were assigned to COG classes. This difference may result from a stronger stress induced by the short-term exposure to salt, as shown by the higher impact salt had on delta growth after 2 $\frac{1}{2}$ h of incubation. It could also possibly be due to distinct global responses induced by the two solutes used to induce osmotic upshifts already shown to be partially conserved in *Sphingomonas* [32].

The distribution of COGs recovered from regulated genes in relation to the total number of COGs in each class is shown in Figure 1. Besides an upregulation of approximately 30% of genes involved in translation ribosomal structure and biogenesis encoding, for example, ribosomal proteins, we found that a majority of genes involved in chemotaxis and motility were repressed by both stresses. Indeed, nearly 60% of genes with COG assigned to that class were repressed upon stress.

Hyperosmotic stresses have already been shown to repress motility gene transcription in many bacteria [32–36] including rhizobia [37]. Interestingly the repression of motility is often associated to an induction of genes involved in the synthesis of biofilm components such as surface polysaccharides or proteins [32,35,38,39].

The regulation of motility genes and surface components have been studied in *Ensifer meliloti* and several transcriptional regulators have been characterized. Regulators such as CbrA, VisN/VisR, and Rem alter the regulation of many genes involved in motility or surface components [40,41], which were shown to be modulated by the ExpR/SinI quorum-sensing system [42], emphasizing the complexity of the regulatory circuits involved. Fine-tuning regulation of motility and cell surface components is of particular importance for bacteria, notably, host-associated ones such as rhizobia that have to adapt to contrasted environments (soil-rhizosphere-nodule) [43]. Among genes that were repressed by the osmotic upshift, VisR/VisN- and Rem-predicted encoding genes (respectively,

PEG655/PEG654 and PEG688) were identified. This may explain the downstream down-regulation of motility genes identified here, even though the repression was less marked under PEG80000 condition, with notably *visR* and *visN* that were less than 2-fold repressed as compared to the control (see Table S1). Even though the design did not enable us to obtain statistical significance on the RNAseq data set, we also found several genes involved in exopolysaccharides to be induced upon salt stress (*exoQ, exoF, exoY exoH, exoO,* and *exoN*, respectively, PEG5904-5906, PEG5914, PEG5919, and PEG5920), supporting a possible developmental switch, as shown in *S. meliloti* [40].

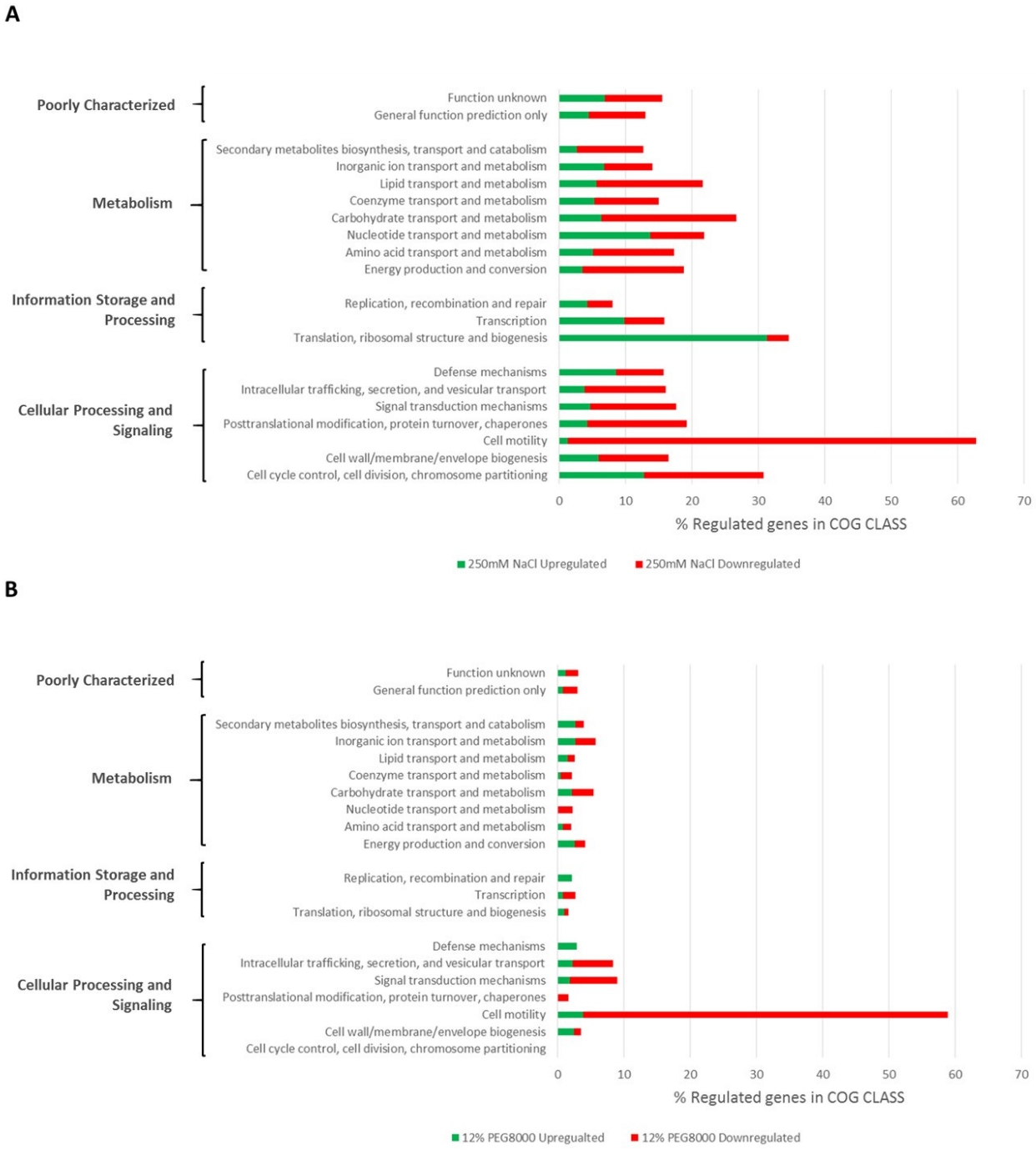

Figure 1. COG-based functional classification of genes regulated (>50× mean coverage and a minimum of 2-fold change) upon salt (**A**) or PEG8000 (**B**) treatments. The horizontal bars represent the % of genes regulated in the corresponding COG Class and, for each bar, the relative proportion of genes that are up- or down-regulated is shown in green and red, respectively. The COG class description and processes to which they belong are shown on the left of graphs.

Among the metabolic pathways known to respond to hyperosmotic stresses, we found that two trehalose de novo biosynthesis pathways were induced. The genes encoding for Alpha,alpha-trehalose-phosphate synthase (*otsA*, PEG4869) and the Trehalose-6-phosphate phosphatase (*otsB*, PEG4868) that converts UDP glucose and glucose 6P into trehalose by two successive reactions were induced more strongly under salt stress (fold changes of 3.7 and 5.2, respectively) than upon PEG8000-induced hyperosmotic stresses (fold changes of 2 and 1.6, respectively). The second pathway that converts maltodextrin to trehalose by a Malto-oligosyltrehalose synthase (*treY*, PEG5229) and a Malto-oligosyltrehalose trehalohydrolase (*treZ*, PEG5323) appeared, in contrast, more induced under PEG treatment with respective fold changes of 4.9 and 4.3 when these were induced 1.8 and 3.4 times by salt. We also found a strong repression of the trehalose ABC-type import system *thuEFGK* (PEG6268, 6266, 6265, and 6264) and the trehalose utilization genes *thuAB* (PEG6263 and 6262), which showed from 9- to 20-fold reduction in expression levels upon salt exposure. These genes were also repressed upon PEG8000 exposure but to a lesser extent (fold changes ranging from 1.5 to 2.7). The induction of trehalose de novo synthesis upon osmotic upshift has been documented in many bacteria, including rhizobia [12,44–46]. *Ensifer aridi* most probably also uses this common non-reducing disaccharide upon osmotic upshift. However, in *Ensifer aridi* LMR001, we found that the ABC-type transport system encoded by *thuEFGK* as well as trehalose catabolic genes *thuAB* [47,48] was strongly repressed, while *thuE*, *thuG*, and *thuA* genes were found induced upon osmotic upshift in *Ensifer meliloti* [37]. This difference may result from different growth media used and, notably, the presence of trehalose in the medium that appears to induce both the *thuEFGK* and *thuAB* genes [47,48]. Interestingly, a repression of the trehalose utilization genes combined with an upregulation of trehalose de novo synthesis should result in increased intracellular trehalose levels that may favor rapid osmo-adaptation to stressful conditions. Interestingly, *S. meliloti* mutants in the *thuAB* genes improved the efficiency of nodulation and, more precisely, the early root hair IT-infection competitiveness [48], which may, however, depend on the host genotype [49]. Symbiotic bacteria that are prone to trehalose biosynthesis such as *E. aridi* may provide advantageous adaptation to plants under abiotic stresses [13].

Among metabolisms that were altered by the salt stress, we found a large locus (PEG2271—PEG2284) shown to be involved in erythritol, adonitol, and L-arabitol transport and catabolism [50]. Predicted genes *eryA* (PEG2278) and *eryB* (PEG2275) showed reduced transcription (respectively, 6.7- and 3.7-fold repression) upon salt exposure, while *eryC* (PEG2271) presented a 2.2-fold repression but a 30× mean coverage. The operon predicted to encode erythritol ABC-type transport system (PEG2283-2279) located just upstream of the catabolic genes was even more strongly repressed by salt (9.5–24-fold repression) when the predicted erythritol transcriptional repressor gene *eryD* (PEG2284) presented a 10-fold repression, which was surprising, as we would expect an induction. Erythritol transport and catabolism was found to be important for nodule occupancy in *Rhizobium leguminosarum* [51] but not in *Sinorhizobium meliloti,* as shown by competitiveness the Triose Phosphate isomerase *tpiB* mutant that cannot utilize erythritol [52]. Given that the erythritol catabolic genes are induced by the presence of erythritol, the repression observed could be due to an increased and rapid utilization of this polyol under salt stress, leading to reduced external erythritol concentration that may also explain the strong repression observed for *thuEFGK* and *thuAB* genes. Other possible explanations may be the involvement of additional transcriptional regulators involved, such as a putative EryR homolog (PEG2270) that was, however, not regulated in the present study or, finally, a possible alternative utilization of an intermediary product of the erythritol catabolism suggested to be involved in its regulation [53].

In contrast to erythritol, inositol transport and metabolism were strongly induced by salt. First a myo-inositol ABC transport system (PEG5305-5307) showed 4.8- to 8.1-fold induction upon salt exposure, as compared to the control treatment. Furthermore, genes encoding 2 myo inositol-2 dehydrogenases *idhA* (PEG2503) and *iolY* (PEG375) that covert, respectively, D-chiro inositol and scyllo-inositol into 2-keto myo-inositol presented salt

inductions (respectively, 6.7- and 1.8-fold changes). The genes *iolE* (PEG371), *iolD* (PEG372), *iolB* (PEG370), and *iolC* (PEG373) that are involved in the successive conversion of 2-keto-myo-inositol into 3-D-trihydroxycyclohexane-1,2-dione, 5-deoxy-glucuronic acid, 2-deoxy-5-keto-D-gluconic acid, and 2-deoxy-5-keto-D-gluconic acid 6-phosphate (DKGP) showed 3.6- to 5.6-fold inductions in the salt treatment, as compared to control. These results support active inositol import and catabolism in salt-treated cells that are under the control of the predicted transcriptional repressor IolR (PEG374). Again, *iolR* was surprisingly also up-regulated by salt with a 2.2-fold induction. It was shown that 2 deoxy 5 keto D gluconic acid 6 P (DKGP), a key product of inositol catabolism, participates in the regulation of many genes involved in this metabolism by interacting with the repressor IolR through competitive binding [54,55], suggesting accumulation of this intermediate product. Interestingly, mutations in genes involved the catabolism of myo-inositol, such as *idhA*, were shown to negatively impact symbiosis development and, particularly, competitiveness for nodule occupancy with their host plants, as shown in *S. meliloti* [56], *S. fredii* [57], and *Rhizobium leguminosarum* bv. *viciae* [58], which suggest involvement of inositol derivatives for proper symbiosis establishment and functioning. The induction of inositol catabolism, together with potential trehalose accumulation, as evidenced by trehalose metabolic and transport genes' expression levels found here upon salt stress together with their respective involvement in symbiosis establishment, further supports a role of such stress-responsive genes in improving symbiosis establishment and functioning [59,60].

We also found an induction by salt stress exposure of genes involved in the methionine cycle. It included the adenosyl homocysteinase *ahcY* (PE3356, 11.4-fold induction) that converts S-adenosyl-L-homocysteine (SAH) into homocysteine that is, in turn, converted to methionine, either from glycine betaine by a betaine–homocysteine S-methyltransferase BHMT (PEG1969, 18.5-fold induction) or from a sequential conversion of 5, 10-methylene tetrahydrofolate by a reductase encoded by *metF* (PEG2238, 4.6-fold induction) to methyl tetrahydrofolate that is converted with homocysteine as substrate into methionine and tetrahydrofolate with a 5-methyltetrahydrofolate-homocysteine methyltransferase by *metH* (PEG3206, 6.7-fold induction). Finally, we found a strong induction (20.5-fold induction by salt) of the S-adenosylmethionine (SAM) synthetase-encoding gene *metK* (PEG438) that converts methionine into SAM, a universal methyl donor used as cofactor in methyl transferase reactions involved in methylation of nucleic acids and protein or in secondary metabolite biosynthesis such as polyamines. Furthermore, two transcriptional factors previously shown to regulate the methionine cycle were also found differentially regulated. The LuxR-type solo *nesR* gene (PEG5735), shown to affect the methionine cycle by Patankar and Gonzalez [61], presented a 2-fold induction upon salt stress, while the *sahR* gene encoding an ArsR-type transcriptional regulator was found 9 times more expressed in the salt condition. SahR was shown to activate several genes of the methionine cycle, including itself upon biding to a SAH, which releases its binding from their promoter, thus enabling their transcriptional activation [62]. An active methionine cycle was shown to be important for osmoprotection in several rhizobia including *S. fredii* [63] or in *S. meliloti* [19,61]. Interestingly, a mutation in *metH*, part of the main pathway for methionine synthesis in *S. meliloti* strain 102F34, or *nesR* in Rm2011 reduced competitiveness for nodule occupancy when the mutants were challenged to the wild type [19,61]. Such observation was also observed in a *metZ* mutant of *R. etli* impaired for methionine biosynthesis when inoculated to *P. vulgaris* [64]. Furthermore, a *cobO* mutant, incapable to biosynthesize the vitamin B12 necessary for MetH-mediated methionine biosynthesis in *S. fredii* HH103, was severely affected in nodulation. Altogether, these data support a role of the methionine in nodulation competitiveness in the rhizobium legume symbiosis and, again, further suggest a possible improvement of symbiosis performance by rhizobial stress-response genes [60].

Salt stress also induced the transcription of the alternative extracytoplasmic function sigma factor *rpoE2* (PEG2539), as well as the anti-sigma factor gene *rsiA1*, a *nepR* homolog (PEG2540), and *rsiB1*, a *phyR* homolog (PEG2541), that were at least induced by 3 folds. This result indicates that the General Stress Response (GSR) was activated in *Ensifer aridi*,

as already shown in other alphaproteobacteria [65]. The effects of mutations in these genes have been studied in various organisms including rhizobial genera, such as *Bradyrhizobium* [66,67], *Sinorhizobium* [68,69], or *Rhizobium* [70], and have shown their involvement as master regulators of the stress response, which may also be found in *Ensifer aridi*. Other regulatory systems have been evidenced, such as the lovK-LovR Two-Component System in *Caulobacter* [71] or in *S. meliloti,* in which homologs of the *rsiA1* and *rsiB1* (anti-sigma and anti-anti-sigma factors, respectively) have recently been shown to modulate *rpoE2* regulation [68]. This shows that the stress response is complex and finely tuned, which is not surprising, as bacteria have to cope with different but sometimes combined stresses, which may utilize common molecular mechanisms depending on the stress. It is interesting to note that we also found homologs of *rsiA1* and *rsiB1,* named, respectively, *rsiA2* (PEG753) and *rsiB2* (PEG752), in our strain, which may act similarly as shown for *S. meliloti.* However, our transcriptomic data showed that the stresses applied here did not affect their transcriptional status, which remained unchanged. Additional studies are required to decipher their regulatory functions. Surprisingly, while bradyrhizobia mutated in genes responsible for the alternative extracytoplasmic function, sigma factor functioning showed strong symbiosis development deficiencies [66,67], symbiosis development and functioning was not impaired by such mutations in *Sinorhizobium meliloti* [69,72] or *Rhizobium etli* [70]. Interestingly, Lang and colleagues [72] demonstrated that the absence of such symbiosis deficiency in *S. meliloti* was not due to extracytoplasmic function sigma factors (ecfG) redundancy. They obtained similar symbiosis phenotypes when all ecfG were mutated and compared to the wild-type strain. Regarding the responses of ecfG mutants to stresses, studies on *S. meliloti* showed contrasting results. In a primary study, Sauviac and colleagues [69] showed that *rpoE2* mutants did not present phenotypic differences with the wild type upon various stresses (heat, salt, acidic pH, or H_2O_2) in both exponential and stationary growth phases. Later, Flechard and colleagues [45,73] showed that a *rpoE2* mutant in a stationary growth phase was sensitive to hydrogen peroxide and hyperosmotic stresses. More recently, Lang and colleagues confirmed Sauviac's results as no or subtle differences were found in the *rpoE2* mutant or a mutant lacking all ECF-like genes, which is surprising, as many stress-responsive genes were identified in the RpoE2 regulon [69,72]. These differences may result from distinct mutation procedures and/or media used in these studies, which included, for example, a deletion of the anti-sigma factors in the study by Lang and colleagues [72]. In *Bradyrhizobium,* such mutations increased sensitivity of *B. japonicum* to heat shock and desiccation [66]. Furthermore, recent work on *B. diazoefficiens* showed that ecfG mutation resulted in increased sensitivity to various stresses including hyperosmotic and ionic stresses [74]. More interestingly, in both *Bradyrhzobium diazoefficiens* and *Sinorhizobium meliloti*, a *rpoE2* mutation was shown to repress trehalose 6 Phosphate pathway, which was involved in hyperosmotic stresses' tolerance [45] and was sufficient to impair early symbiotic development in the more sensitive *B. diazoefficiens* species [74], further supporting that trehalose is a key compatible solute for *Bradyrhizobium* stress adaptation and nodulation, as shown in *B. japonicum* [46]. The absence of a symbiotic phenotype observed in the *rpoE2* mutant of *S. meliloti* may result from a high tolerance to hyperosmotic stress in this species as compared to the *Bradyrhizobium* species. Such stress may be encountered, notably, in infection threads, which is supported by the restoration of symbiosis by addition of exogenous trehalose in *B. diazoefficiens* Δ*otsA* strain still capable to import it or in a strain capable to endogenously synthesize other compatible osmoprotectants [74]. To explore the function of RpoE2 and its possible role in the regulation of several functions shown to be transcriptionally regulated by salt stress as well as in the tolerance of the LMR001 bacterium to various stresses and symbiosis development, a deletion mutant of the *rpoE2* gene (Δ*rpoE2*) was generated and phenotypically characterized.

First, the growth of Δ*rpoE2* was compared to that of LMR001 in TY medium complemented with salt at 250, 300, and 400 mM final concentrations (Figure 2A). We found that, even though the WT strain reached the stationary phase earlier in TY medium containing 250 mM of NaCl as compared to Δ*rpoE2*, both strains reached comparable optical densities

after 120 h of incubation. Secondly, when we looked at the motility of the two strains, while we found a significant reduction of motility for the two strains upon addition of salt at both concentrations tested (0.1 and 0.25 M), which corroborates transcriptional data observed by RNAseq, no clear differences were observed between the two strains (Figure 2B). Sensitivities of the two strains to detergent, oxidative, and acid stresses were estimated by the inhibitory growth diameter induced by the diffusion in the agar medium of 5 µL concentrated SDS, H_2O_2, or HCl that were spotted on small paper discs placed in the center of soft agar plates previously inoculated with the strains (see Materials and Methods). The concentration of these molecules decreased as they diffused away from the discs imbibed with the reagents. A measure of the growth inhibition diameter, thus, enabled us to compare tolerance of the strains. We did not find any difference between the wild-type and the Δ*rpoE2* strains (Figure 2C), suggesting that the *rpoE2* mutation did not alter cell membrane stability under such stresses. Finally, both the LMR001 and Δ*rpoE2* strains developed the symbiosis with the tree species *V. gummifera* and *V. tortilis* and there were no significant differences associated to plant weights or nodulation (Table 2). These results show that the ECF sigma factor RpoE2 is not essential for motility, symbiosis development, and tolerance to the stresses tested, suggesting that other functions and/or regulators are involved in these processes, as suggested in *Sinorhizobium meliloti* [69,72].

We further explored the involvement of the extra cytoplasmic function sigma factor in the transcriptional regulation of genes involved in the inositol catabolism (*iolC* and *iolR*), methionine cycle regulation (*nesR* and *sahR*), trehalose transport, and metabolism (*thuR*, *thuE*, *otsB*, and *treZ*) including a glycosyl transferase (PEG4866) located upstream of the *otsBA* operon in reverse orientation or in the regulation of the GSR (*rsiA1*, *rsiB1*). Their promoter regions were fused in front of the reporter gene encoding GFP in a mobilizable vector, and resulting constructions were further transferred into LMR001 and Δ*rpoE2*. Both strains containing the pPROBE derivatives were then grown either in TY medium or in TY complemented with NaCl at a final concentration of 250 mM in 96-microtiter plates and fluorescence with the optical density (600 nm) and were recorded every half hour.

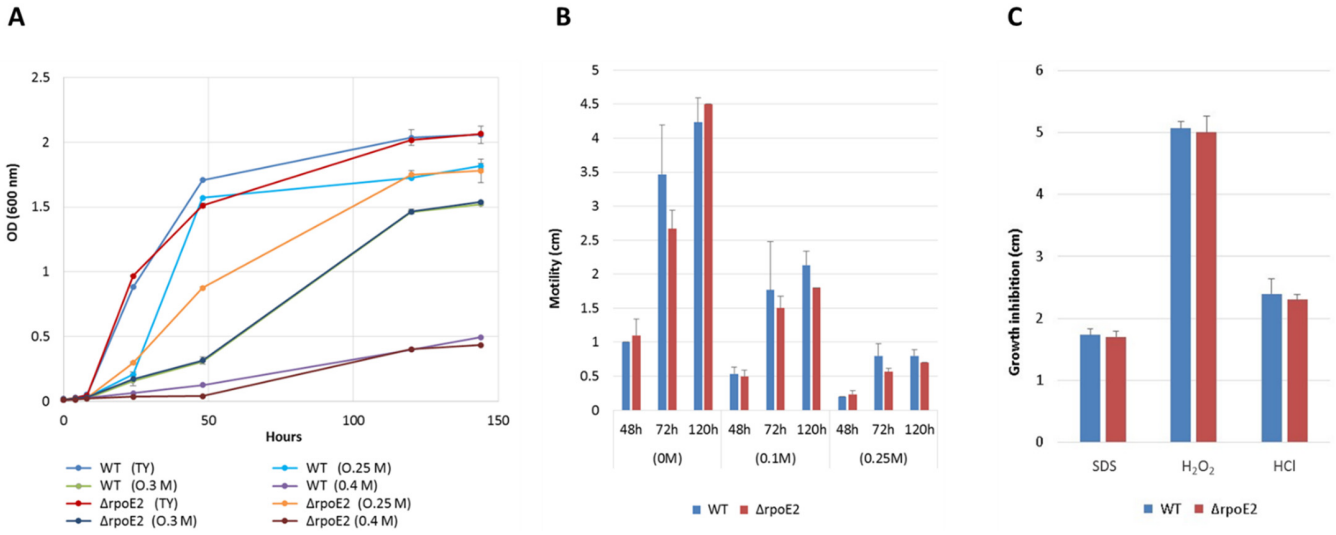

Figure 2. Effect of the rpoE2 mutation on stress tolerance and motility of LMR001. *Ensifer aridi* LMR001 (WT) and the LMR001 *rpoE2* deletion mutant (ΔrpoE2) growths were compared in liquid TY medium complemented with 0, 0.1, 0.25, 0.3, or 0.4 M of NaCl (**A**). Their motility was assessed in semi-solid TY complemented with salt at 0, 0.1, or 0.25 M by measurement of the diameter of the swimming colonies after 2, 3, or 5 days of incubation (**B**). Finally, the diameters of the growth inhibition zones were compared for the two strains inoculated in top agar plates, to the center of which patches imbued with 5 µL of SDS (10% *w*/*v*), H_2O_2 (5.5 M), or HCl (2 M) were placed (**C**).

Table 2. Effect of the *rpoE2* mutation on symbiosis development with *Vachellia*.

Plant/Treatment	Shoot Weight (g)		Root Weight (g)		Nodule Number	
	Mean	*Standard Deviation*	Mean	*Standard Deviation*	Mean	*Standard Deviation*
Vachellia gummifera						
LMR001 WT	2.27	0.21	0.90	0.09	33	3.22
LMR001 Δ*rpoE2*	2.33	0.37	1.03	0.19	35.67	5.24
Positive Control	3.13	0.10	2.83	0.26	0	
Negative Control	1.37	0.14	1.07	0.10	0	
Vachellia tortilis						
LMR001 WT	2.72	0.09	0.83	0.05	39	1.79
LMR001 Δ*rpoE2*	2.16	0.21	1.08	0.15	38	3.94
Positive Control	3.73	0.58	2.33	0.26	0	
Negative Control	1.83	0.14	1.10	0.09	0	

Figure 3 shows the relative expression levels of the GFP under the control of selected promoters recorded every 30 min for 9 h. The relative expression of the GFP varied with the promoter and, for some of them, with the strain. The approach did not allow us to detect differences between salt and control growth conditions for a strain that would require less stable GFP and a more sensitive approach to detect early response to hyperosmotic stress. However, the methodology enabled us to identify transcriptional changes resulting from the mutation. We found that the mutation resulted in an increased transcription of four genes, while it reduced the expression of three genes. An increased transcription of *otsB* was obtained in the Δ*rpoE2* strain, indicating that RpoE2-mediated GSR in *E. aridi* involves the T6P pathway, as shown in *S. meliloti* [45] or in *B. diazoefficiens* [74]. We also found that for *rsiA1,* the anti-sigma factor that is located upstream of and overlaps the 5′ end of the *rpoE2* gene forming an operon was less expressed in the mutant, which suggests, again, that, as shown in other alphaproteobacteria [65], *rpoE2* is autoregulated in *E. aridi*. Given the high similarities, both in terms of syntheny and sequence between *S. meliloti* and *E. aridi* for many genes discussed here (for example, 97.8% similarity for RpoE2), we tested whether the same promoter motif $GGAACN_{16\text{-}17}CGTT$ that likely represents the −35 and −10 elements of the RpoE2 responsive genes [69,72] could be found in the target promoter sequences of *E. aridi* genes studied here. This motif was found upstream of *rsiA1* and *rsiB1,* supporting a conserved RpoE2-mediated regulatory mechanism. It was also found twice in the promoter region of the *treZ* gene, whose transcription was, however, not found significantly different when comparing the WT and Δ*rpoE2* strains, and in the range of background values. Regarding the *otsB* promoter region, we found two motifs that were close to the consensus sequence: ($GGAACN_{17}CGAT$ and $AGAACN_{17}CGAT$). Finally, one motif with three nucleotide differences as compared to the consensus sequence was found in front of the *thuR* gene ($GGAAAN_{17}AGAT$). However, the involvement of these regions requires additional work to assess whether these are directly regulated by RpoE2 and to exclude the possibility that a hidden mutation resulting from the mutagenesis impacted our data. Surprisingly, the most severe transcriptional repression resulting from the mutation was found for *thuR*, encoding a HTH DNA-Binding LacI-type repressor showing homologies to *aglR* that may be involved in transport and utilization of trehalose through *thuEFGK* and *thuAB* expression [47,48]. It is interesting to note the presence of *thuR* consensus sequence motifs found among rhizobiales upstream of these operons in LMR001 as well as in front of *aglR* and *aglEFGAK* that share partially their motifs [75], which may, however, explain cross-regulation of these transport systems by *aglR* [47]. Given (1) ThuR homology to AglR, (2) the trehalose transport specificity observed of ThuE, ThuF, ThuG, and ThuK, shown by Jensen and colleagues, and (3) evolutionary and comparative analyses within rhizobiales of LacI-family transcription factors that predicts ThuR as a regulator of two operons (*thuEFGKAB* involved in trehalose transport and utilization as well as *thuR*) [47,75], our data further support that ThuR is also autoregulated and involved in the regulation of transport and utilization of trehalose in *E. aridi*. Nevertheless, additional

work is required to characterize the regulatory pathways involved and, notably, whether *thuR* is directly or indirectly regulated by RpoE2.

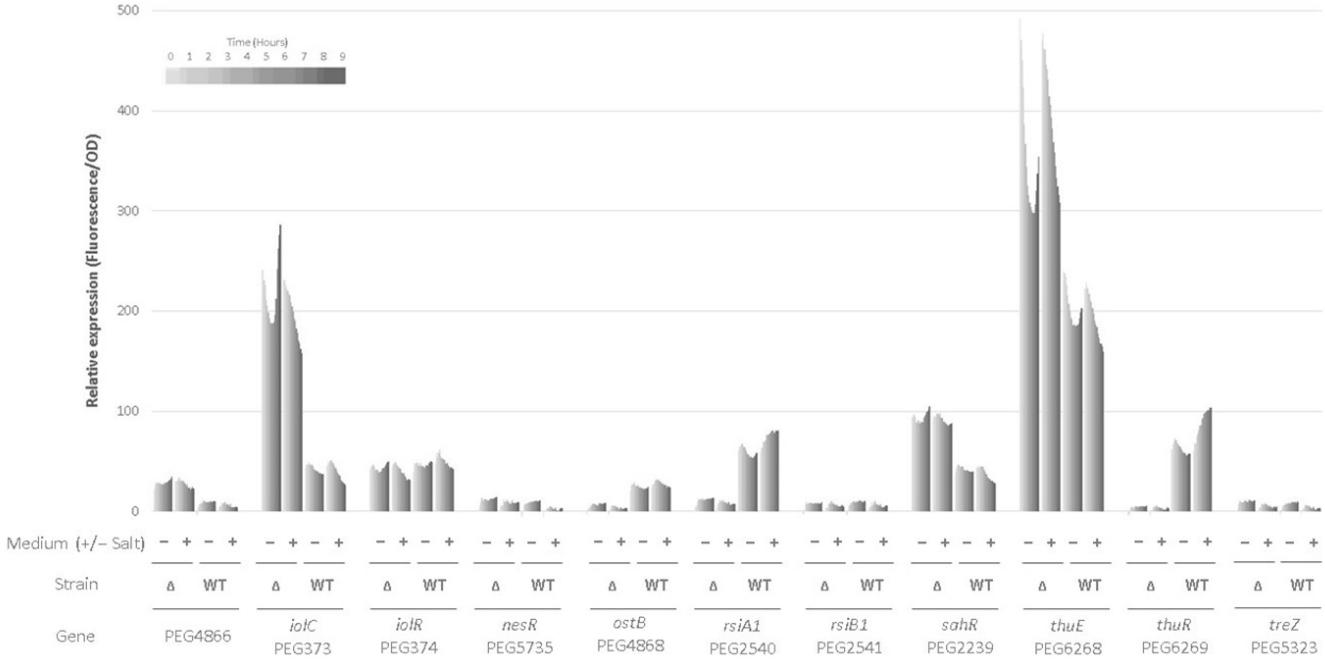

Figure 3. Effect of the *rpoE2* mutation on transcriptional activity of selected genes. The histograms show the relative expression (see Materials and Methods) of *gfp* under the control of promoters from selected genes mobilized in wild-type *Ensifer aridi* LMR001 (WT) or the Δ*rpoE2* derivative (Δ) strains grown in TY medium containing salt (NaCl at 250 mM) or not (+/−), as indicated at the bottom of the figure. Relative expressions were recorded every 30 min for 9 h and are shown by gray bars of increasing darkness with time (colors indicated on the top left of the figure).

Among genes whose transcriptional activities were increased by the mutation, we found *thuE,* which may result from the *thuR* repression in the Δ*rpoE2* strain. Interestingly, the glycosyl transferase (PEG4866) located upstream of the *otsBA* operon in reverse orientation also showed an increased transcriptional activity in Δ*rpoE2,* which may suggest RpoE2-mediated repression in the wild-type strain. Surprisingly, *iolC* and *sahR* genes involved, respectively, in the catabolism of myo-inositol and the regulation of the methionine cycle were also found more expressed in Δ*rpoE2* background while they were found induced upon salt stress in the wild-type LMR001 strain. Whether these inductions result from a direct RpoE2-mediated repression remains to be addressed, but our data suggest a complex stress response in *E. aridi,* which involves RpoE2 that can, nevertheless, be complemented.

4. Conclusions

To explore the mechanisms by which *Ensifer aridi* LMR001 copes with hyperosmotic stresses, 31 Gb of sequence data were generated by three RNAseq libraries constructed from cells grown either in control medium or upon addition of the permeating solute NaCl at 250 mM or the non-permeating solute PEG8000 at 12% *w*/*v*. As shown in other bacteria, hyperosmotic stresses resulted in the repression of motility genes, which was confirmed by phenotypic tests. These effects may be considered for improving the rhizobium–legume symbiosis in soils containing salt, notably, through inoculation of adapted bacteria to ensure contact between non-motile rhizobia and roots. We also found that the extra-cytoplasmic function sigma factor-encoding gene *rpoE2* was induced and probably involved, as shown in other rhizobia, in its autoregulation and the induction of trehalose de novo biosynthesis. A concomitant repression of trehalose utilization genes *thuAB* suggests intracellular accumulation of trehalose in stressed cells. Salt also induced inositol catabolism and the

methionine cycle, suggesting a possible role of inositol derivatives and possibly methylation in the early response to such stress. In addition, a combination of directed mutagenesis of *rpoE2* and the use of promoter-*gfp* fusion reporter system suggested that RpoE2 regulates positively *thuR*, a LacI-type regulator probably involved in trehalose import and utilization. In contrast, the mutation resulted in increased expression of genes involved in inositol catabolism or the regulation of the methionine cycle that, given their induction in the wild-type bacterium upon salt stress, supports the involvement of alternative regulatory circuits. However, additional experiments are required to ascertain that Δ*rpoE2* does not carry hidden mutations, which could have impacted our data. Intriguingly, previous studies showed that a mutation of trehalose utilization genes in *S. meliloti* resulted in improved competitiveness for nodulation, which is also favored with active inositol catabolism and methionine cycle, suggesting that hyperosmotic stress occurs in the early infection of leguminous hosts. The *rpoE2* deletion did not result in increased stress sensitivity or symbiosis functioning, suggesting the involvement of alternative regulatory circuits in *Ensifer aridi* for stress adaptation.

Supplementary Materials: The following are available online at https://www.mdpi.com/article/10.3390/agronomy11091787/s1. Figure S1: Sequencing and mapping of the three RNAseq libraries. Figure S2: Distributions of RNAseq data. Figure S3: Effect of PEG order, mean coverage, or size on the relative abundance of reads obtained in the three libraries. Figure S4: Comparison of the relative expression levels of selected genes by RNAseq and qPCR. Table S1: Predicted LMR001-encoding gene annotation and mapping.

Author Contributions: Conceptualization, A.L.Q. and A.F.-M.; methodology, A.L.Q., M.B., E.D., D.S. and H.A.-B.; formal analysis, M.B. and A.L.Q.; investigation, M.B., A.L.Q. and I.S.; resources, E.D. and D.S.; data curation, E.D., D.S. and A.L.Q.; writing—original draft preparation, M.B. and A.L.Q.; writing—review and editing, all authors.; visualization, A.L.Q. and M.B.; supervision, A.L.Q. and A.F.-M.; project administration, A.L.Q. and A.F.-M.; funding acquisition, A.L.Q. and A.F.-M. All authors have read and agreed to the published version of the manuscript.

Funding: This research was funded by the French Institute of Research for the Development (IRD) through the LMI LBMV and an ARTS PhD grant for M.B.

Institutional Review Board Statement: Not applicable.

Informed Consent Statement: Not applicable.

Data Availability Statement: *Ensifer aridi* LMR001 genome browser, Fasta nucleotide and protein sequences and annotations can be accessed through the RAST server https://rast.nmpdr.org/ (accessed 11 November 2020) using "guest" as login and password under job nb "188440" with ID "6666666.88372". RNAseq data have been deposited in SRA in NCBI and can be accessed through the Bioproject PRJNA312299.

Acknowledgments: The authors would like to acknowledge Samir El Qaidi for methodological support for the construction of the mutant and Abderrahim Ferradous from the Centre Régional de Recherches Forestière in Marrakech for *Vachellia* seeds. M.G.X. acknowledges financial support from France Génomique National infrastructure, funded as part of "Investissement d'Avenir" program managed by Agence Nationale pour la Recherche (contract ANR-10-INBS-09).

Conflicts of Interest: The authors declare no conflict of interest. The funders had no role in the design of the study; in the collection, analyses, or interpretation of data; in the writing of the manuscript; or in the decision to publish the results.

References

1. Sakrouhi, I.; Belfquih, M.; Sbabou, L.; Moulin, P.; Bena, G.; Filali-Maltouf, A.; Le Quéré, A. Recovery of Symbiotic Nitrogen Fixing Acacia Rhizobia from Merzouga Desert Sand Dunes in South East Morocco—Identification of a Probable New Species of *Ensifer* Adapted to Stressed Environments. *Syst. Appl. Microbiol.* **2016**, *39*, 122–131. [CrossRef]
2. Rocha, G.; Le Queré, A.; Medina, A.; Cuéllar, A.; Contreras, J.-L.; Carreño, R.; Bustillos, R.; Muñoz-Rojas, J.; Villegas, M. del C.; Chaintreuil, C.; et al. Diversity and Phenotypic Analyses of Salt- and Heat-Tolerant Wild Bean *Phaseolus filiformis* Rhizobia Native of a Sand Beach in Baja California and Description of *Ensifer aridi* Sp. Nov. *Arch. Microbiol.* **2020**, *202*, 309–322. [CrossRef] [PubMed]

3. Tak, N.; Awasthi, E.; Bissa, G.; Meghwal, R.R.; James, E.K.; Sprent, J.S.; Gehlot, H.S. Multi Locus Sequence Analysis and Symbiotic Characterization of Novel *Ensifer* Strains Nodulating *Tephrosia* Spp. in the Indian Thar Desert. *Syst. Appl. Microbiol.* **2016**, *39*, 534–545. [CrossRef] [PubMed]
4. Hakim, S.; Imran, A.; Mirza, M.S. Phylogenetic Diversity Analysis Reveals *Bradyrhizobium yuanmingense* and *Ensifer aridi* as Major Symbionts of Mung Bean (*Vigna radiata* L.) in Pakistan. *Braz. J. Microbiol.* **2021**, *52*, 311–324. [CrossRef] [PubMed]
5. Lamin, H.; Alami, S.; Bouhnik, O.; ElFaik, S.; Abdelmoumen, H.; Bedmar, E.J.; Missbah-El Idrissi, M. Nodulation of *Retama monosperma* by *Ensifer aridi* in an Abandonned Lead Mine Soils in Eastern Morocco. *Front. Microbiol.* **2019**, *10*, 1456. [CrossRef]
6. Le Quéré, A.; Tak, N.; Gehlot, H.S.; Lavire, C.; Meyer, T.; Chapulliot, D.; Rathi, S.; Sakrouhi, I.; Rocha, G.; Rohmer, M.; et al. Genomic Characterization of *Ensifer aridi*, a Proposed New Species of Nitrogen-Fixing Rhizobium Recovered from Asian, African and American Deserts. *BMC Genom.* **2017**, *18*, 85. [CrossRef] [PubMed]
7. Zahran, H.H. *Rhizobium* -Legume Symbiosis and Nitrogen Fixation under Severe Conditions and in an Arid Climate. *Microbiol. Mol. Biol. Rev.* **1999**, *63*, 968–989. [CrossRef]
8. Denich, T.J.; Beaudette, L.A.; Lee, H.; Trevors, J.T. Effect of Selected Environmental and Physico-Chemical Factors on Bacterial Cytoplasmic Membranes. *J. Microbiol. Methods* **2003**, *52*, 149–182. [CrossRef]
9. Chang, W.-S.; van de Mortel, M.; Nielsen, L.; Nino de Guzman, G.; Li, X.; Halverson, L.J. Alginate Production by *Pseudomonas putida* Creates a Hydrated Microenvironment and Contributes to Biofilm Architecture and Stress Tolerance under Water-Limiting Conditions. *J. Bacteriol.* **2007**, *189*, 8290–8299. [CrossRef]
10. Finn, S.; Condell, O.; McClure, P.; Amézquita, A.; Fanning, S. Mechanisms of Survival, Responses and Sources of *Salmonella* in Low-Moisture Environments. *Front. Microbiol.* **2013**, *4*, 331. [CrossRef]
11. Lebre, P.H.; De Maayer, P.; Cowan, D.A. Xerotolerant Bacteria: Surviving through a Dry Spell. *Nat. Rev. Microbiol.* **2017**, *15*, 285–296. [CrossRef]
12. Vriezen, J.A.C.; de Bruijn, F.J.; Nüsslein, K. Responses of Rhizobia to Desiccation in Relation to Osmotic Stress, Oxygen, and Temperature. *Appl. Environ. Microbiol.* **2007**, *73*, 3451–3459. [CrossRef]
13. Sharma, M.P.; Grover, M.; Chourasiya, D.; Bharti, A.; Agnihotri, R.; Maheshwari, H.S.; Pareek, A.; Buyer, J.S.; Sharma, S.K.; Schütz, L.; et al. Deciphering the Role of Trehalose in Tripartite Symbiosis Among Rhizobia, Arbuscular Mycorrhizal Fungi, and Legumes for Enhancing Abiotic Stress Tolerance in Crop Plants. *Front. Microbiol.* **2020**, *11*, 509919. [CrossRef] [PubMed]
14. Bonilla, C.Y. Generally Stressed Out Bacteria: Environmental Stress Response Mechanisms in Gram-Positive Bacteria. *Integr. Comp. Biol.* **2020**, *60*, 126–133. [CrossRef]
15. Fiebig, A.; Herrou, J.; Willett, J.; Crosson, S. General Stress Signaling in the *Alphaproteobacteria*. *Annu. Rev. Genet.* **2015**, *49*, 603–625. [CrossRef]
16. Lori, C.; Kaczmarczyk, A.; de Jong, I.; Jenal, U. A Single-Domain Response Regulator Functions as an Integrating Hub To Coordinate General Stress Response and Development in *Alphaproteobacteria*. *mBio* **2018**, *9*, e00809-18. [CrossRef]
17. Beringer, J.E. R Factor Transfer in *Rhizobium leguminosarum*. *Microbiology* **1974**, *84*, 188–198. [CrossRef] [PubMed]
18. Sambrook, J.; Fritsch, E.; Maniatis, T. *Molecular Cloning: A Laboratory Manual*, 2nd ed.; Cold Spring Harbor: New York, NY, USA, 1989; Volume 2, ISBN 978-0-87969-309-1.
19. Barra, L.; Fontenelle, C.; Ermel, G.; Trautwetter, A.; Walker, G.C.; Blanco, C. Interrelations between Glycine Betaine Catabolism and Methionine Biosynthesis in *Sinorhizobium meliloti* Strain 102F34. *J. Bacteriol.* **2006**, *188*, 7195–7204. [CrossRef]
20. Broughton, W.J.; Dilworth, M.J. Control of Leghaemoglobin Synthesis in Snake Beans. *Biochem. J.* **1971**, *125*, 1075–1080. [CrossRef] [PubMed]
21. Maynaud, G.; Brunel, B.; Mornico, D.; Durot, M.; Severac, D.; Dubois, E.; Navarro, E.; Cleyet-Marel, J.-C.; Le Quéré, A. Genome-Wide Transcriptional Responses of Two Metal-Tolerant Symbiotic *Mesorhizobium* Isolates to Zinc and Cadmium Exposure. *BMC Genom.* **2013**, *14*, 292. [CrossRef] [PubMed]
22. Kanehisa, M.; Goto, S.; Sato, Y.; Kawashima, M.; Furumichi, M.; Tanabe, M. Data, Information, Knowledge and Principle: Back to Metabolism in KEGG. *Nucl. Acids Res.* **2014**, *42*, D199–D205. [CrossRef]
23. Tatusov, R.L. The COG Database: New Developments in Phylogenetic Classification of Proteins from Complete Genomes. *Nucl. Acids Res.* **2001**, *29*, 22–28. [CrossRef]
24. Pfaffl, M.W. A New Mathematical Model for Relative Quantification in Real-Time RT-PCR. *Nucl. Acids Res.* **2001**, *29*, e45. [CrossRef] [PubMed]
25. Chen, W.; Kuo, T. A Simple and Rapid Method for the Preparation of Gram-Negative Bacterial Genomic DNA. *Nucl. Acids Res.* **1993**, *21*, 2260. [CrossRef]
26. Quandt, J.; Hynes, M.F. Versatile Suicide Vectors Which Allow Direct Selection for Gene Replacement in Gram-Negative Bacteria. *Gene* **1993**, *127*, 15–21. [CrossRef]
27. Simon, R.; Priefer, U.; Pühler, A. A Broad Host Range Mobilization System for In Vivo Genetic Engineering: Transposon Mutagenesis in Gram Negative Bacteria. *Nat. Biotechnol.* **1983**, *1*, 784–791. [CrossRef]
28. Miller, W.G.; Leveau, J.H.J.; Lindow, S.E. Improved *Gfp* and *InaZ* Broad-Host-Range Promoter-Probe Vectors. *Mol. Plant Microbe Interact.* **2000**, *13*, 1243–1250. [CrossRef] [PubMed]
29. An, Z.; Wang, Q.; Hu, Y.; Zhao, Y.; Li, Y.; Cheng, H.; Huang, H. Co-Extraction of High-Quality RNA and DNA from Rubber Tree (*Hevea brasiliensis*). *Afr. J. Biotechnol.* **2012**, *11*, 9308–9314. [CrossRef]

30. Roose-Amsaleg, C.L.; Garnier-Sillam, E.; Harry, M. Extraction and Purification of Microbial DNA from Soil and Sediment Samples. *Appl. Soil Ecol.* **2001**, *18*, 47–60. [CrossRef]
31. Anders, S.; Huber, W. Differential Expression Analysis for Sequence Count Data. *Genome Biol.* **2010**, *11*, R106. [CrossRef]
32. Alavi, P.; Starcher, M.R.; Zachow, C.; Müller, H.; Berg, G. Root-Microbe Systems: The Effect and Mode of Interaction of Stress Protecting Agent (SPA) *Stenotrophomonas rhizophila* DSM14405T. *Front. Plant Sci.* **2013**, *4*, 141. [CrossRef] [PubMed]
33. Dressaire, C.; Moreira, R.N.; Barahona, S.; Alves de Matos, A.P.; Arraiano, C.M. BolA Is a Transcriptional Switch That Turns Off Motility and Turns On Biofilm Development. *mBio* **2015**, *6*, e02352-14. [CrossRef]
34. Li, S.; Liang, H.; Wei, Z.; Bai, H.; Li, M.; Li, Q.; Qu, M.; Shen, X.; Wang, Y.; Zhang, L. An Osmoregulatory Mechanism Operating through OmpR and LrhA Controls the Motile-Sessile Switch in the Plant Growth-Promoting Bacterium *Pantoea alhagi*. *Appl. Environ. Microbiol.* **2019**, *85*, e00077-19. [CrossRef] [PubMed]
35. Steil, L.; Hoffmann, T.; Budde, I.; Völker, U.; Bremer, E. Genome-Wide Transcriptional Profiling Analysis of Adaptation of *Bacillus subtilis* to High Salinity. *J. Bacteriol.* **2003**, *185*, 6358–6370. [CrossRef]
36. Zhou, A.; Baidoo, E.; He, Z.; Mukhopadhyay, A.; Baumohl, J.K.; Benke, P.; Joachimiak, M.P.; Xie, M.; Song, R.; Arkin, A.P.; et al. Characterization of NaCl Tolerance in *Desulfovibrio vulgaris* Hildenborough through Experimental Evolution. *ISME J.* **2013**, *7*, 1790–1802. [CrossRef] [PubMed]
37. Domínguez-Ferreras, A.; Pérez-Arnedo, R.; Becker, A.; Olivares, J.; Soto, M.J.; Sanjuán, J. Transcriptome Profiling Reveals the Importance of Plasmid PSymB for Osmoadaptation of *Sinorhizobium meliloti*. *J. Bacteriol.* **2006**, *188*, 7617–7625. [CrossRef] [PubMed]
38. Bahlawane, C.; McIntosh, M.; Krol, E.; Becker, A. *Sinorhizobium meliloti* Regulator MucR Couples Exopolysaccharide Synthesis and Motility. *Mol. Plant Microbe Interact.* **2008**, *21*, 1498–1509. [CrossRef] [PubMed]
39. Liu, Y.; Gao, W.; Wang, Y.; Wu, L.; Liu, X.; Yan, T.; Alm, E.; Arkin, A.; Thompson, D.K.; Fields, M.W.; et al. Transcriptome Analysis of *Shewanella oneidensis* MR-1 in Response to Elevated Salt Conditions. *J. Bacteriol.* **2005**, *187*, 2501–2507. [CrossRef] [PubMed]
40. Gibson, K.E.; Barnett, M.J.; Toman, C.J.; Long, S.R.; Walker, G.C. The Symbiosis Regulator CbrA Modulates a Complex Regulatory Network Affecting the Flagellar Apparatus and Cell Envelope Proteins. *J. Bacteriol.* **2007**, *189*, 3591–3602. [CrossRef]
41. Sourjik, V.; Muschler, P.; Scharf, B.; Schmitt, R. VisN and VisR Are Global Regulators of Chemotaxis, Flagellar, and Motility Genes in *Sinorhizobium (Rhizobium) meliloti*. *J. Bacteriol.* **2000**, *182*, 782–788. [CrossRef] [PubMed]
42. Hoang, H.H.; Gurich, N.; González, J.E. Regulation of Motility by the ExpR/Sin Quorum-Sensing System in *Sinorhizobium meliloti*. *J. Bacteriol.* **2008**, *190*, 861–871. [CrossRef]
43. Janczarek, M. Environmental Signals and Regulatory Pathways That Influence Exopolysaccharide Production in Rhizobia. *Int. J. Mol. Sci.* **2011**, *12*, 7898–7933. [CrossRef]
44. Domínguez-Ferreras, A.; Soto, M.J.; Pérez-Arnedo, R.; Olivares, J.; Sanjuán, J. Importance of Trehalose Biosynthesis for *Sinorhizobium meliloti* Osmotolerance and Nodulation of Alfalfa Roots. *J. Bacteriol.* **2009**, *191*, 7490–7499. [CrossRef]
45. Flechard, M.; Fontenelle, C.; Blanco, C.; Goude, R.; Ermel, G.; Trautwetter, A. RpoE2 of *Sinorhizobium meliloti* Is Necessary for Trehalose Synthesis and Growth in Hyperosmotic Media. *Microbiology* **2010**, *156*, 1708–1718. [CrossRef]
46. Sugawara, M.; Cytryn, E.J.; Sadowsky, M.J. Functional Role of *Bradyrhizobium Japonicum* Trehalose Biosynthesis and Metabolism Genes during Physiological Stress and Nodulation. *Appl. Environ. Microbiol.* **2010**, *76*, 1071–1081. [CrossRef] [PubMed]
47. Jensen, J.B.; Peters, N.K.; Bhuvaneswari, T.V. Redundancy in Periplasmic Binding Protein-Dependent Transport Systems for Trehalose, Sucrose, and Maltose in *Sinorhizobium meliloti*. *J. Bacteriol.* **2002**, *184*, 2978–2986. [CrossRef] [PubMed]
48. Jensen, J.B.; Ampomah, O.Y.; Darrah, R.; Peters, N.K.; Bhuvaneswari, T.V. Role of Trehalose Transport and Utilization in *Sinorhizobium meliloti*–Alfalfa Interactions. *Mol. Plant Microbe Interact.* **2005**, *18*, 694–702. [CrossRef] [PubMed]
49. Ampomah, O.Y.; Jensen, J.B.; Bhuvaneswari, T.V. Lack of Trehalose Catabolism in *Sinorhizobium* Species Increases Their Nodulation Competitiveness on Certain Host Genotypes. *New Phytol.* **2008**, *179*, 495–504. [CrossRef]
50. Geddes, B.A.; Oresnik, I.J. Genetic Characterization of a Complex Locus Necessary for the Transport and Catabolism of Erythritol, Adonitol and l-Arabitol in *Sinorhizobium meliloti*. *Microbiology* **2012**, *158*, 2180–2191. [CrossRef] [PubMed]
51. Yost, C.K.; Rath, A.M.; Noel, T.C.; Hynes, M.F. Characterization of Genes Involved in Erythritol Catabolism in *Rhizobium leguminosarum* Bv. *viciae*. *Microbiology* **2006**, *152*, 2061–2074. [CrossRef] [PubMed]
52. Poysti, N.J.; Oresnik, I.J. Characterization of *Sinorhizobium meliloti* Triose Phosphate Isomerase Genes. *J. Bacteriol.* **2007**, *189*, 3445–3451. [CrossRef]
53. Geddes, B.A.; Pickering, B.S.; Poysti, N.J.; Collins, H.; Yudistira, H.; Oresnik, I.J. A Locus Necessary for the Transport and Catabolism of Erythritol in *Sinorhizobium meliloti*. *Microbiology* **2010**, *156*, 2970–2981. [CrossRef]
54. Kohler, P.R.A.; Choong, E.-L.; Rossbach, S. The RpiR-Like Repressor IolR Regulates Inositol Catabolism in *Sinorhizobium meliloti*. *J. Bacteriol.* **2011**, *193*, 5155–5163. [CrossRef]
55. Herrou, J.; Crosson, S. *Myo* -Inositol and D-Ribose Ligand Discrimination in an ABC Periplasmic Binding Protein. *J. Bacteriol.* **2013**, *195*, 2379–2388. [CrossRef] [PubMed]
56. Kohler, P.R.A.; Zheng, J.Y.; Schoffers, E.; Rossbach, S. Inositol Catabolism, a Key Pathway in *Sinorhizobium meliloti* for Competitive Host Nodulation. *Appl. Environ. Microbiol.* **2010**, *76*, 7972–7980. [CrossRef] [PubMed]
57. Jiang, G.; Krishnan, A.H.; Kim, Y.-W.; Wacek, T.J.; Krishnan, H.B. A Functional *Myo* -Inositol Dehydrogenase Gene Is Required for Efficient Nitrogen Fixation and Competitiveness of *Sinorhizobium fredii* USDA191 To Nodulate Soybean (*Glycine max* [L.] Merr.). *J. Bacteriol.* **2001**, *183*, 2595–2604. [CrossRef] [PubMed]

58. Fry, J.; Wood, M.; Poole, P.S. Investigation of *Myo* -Inositol Catabolism in *Rhizobium leguminosarum* Bv. *viciae and Its Effect on Nodulation Competitiveness. Mol. Plant Microbe Interact.* **2001**, *14*, 1016–1025. [CrossRef] [PubMed]
59. Gourion, B.; Berrabah, F.; Ratet, P.; Stacey, G. Rhizobium–Legume Symbioses: The Crucial Role of Plant Immunity. *Trends Plant Sci.* **2015**, *20*, 186–194. [CrossRef]
60. Rodrigo da-Silva, J.; Alexandre, A.; Brígido, C.; Oliveira, S. Can Stress Response Genes Be Used to Improve the Symbiotic Performance of Rhizobia? *AIMS Microbiol.* **2017**, *3*, 365–382. [CrossRef]
61. Patankar, A.V.; González, J.E. An Orphan LuxR Homolog of *Sinorhizobium meliloti* Affects Stress Adaptation and Competition for Nodulation. *Appl. Environ. Microbiol.* **2009**, *75*, 946–955. [CrossRef]
62. Novichkov, P.S.; Li, X.; Kuehl, J.V.; Deutschbauer, A.M.; Arkin, A.P.; Price, M.N.; Rodionov, D.A. Control of Methionine Metabolism by the SahR Transcriptional Regulator in Proteobacteria: Control of Methionine Metabolism in Proteobacteria. *Environ. Microbiol.* **2014**, *16*, 1–8. [CrossRef]
63. Jiang, J.Q.; Wei, W.; Du, B.H.; Li, X.H.; Wang, L.; Yang, S.S. Salt-Tolerance Genes Involved in Cation Efflux and Osmoregulation of *Sinorhizobium fredii* RT19 Detected by Isolation and Characterization of Tn5 Mutants. *FEMS Microbiol. Lett.* **2004**, *239*, 139–146. [CrossRef]
64. Taté, R.; Riccio, A.; Caputo, E.; laccarino, M.; Patriarca, E.J. The *Rhizobium etli metZ* Gene Is Essential for Methionine Biosynthesis and Nodulation of *Phaseolus vulgaris*. *Mol. Plant Microbe Interact.* **1999**, *12*, 24–34. [CrossRef] [PubMed]
65. Francez-Charlot, A.; Kaczmarczyk, A.; Fischer, H.-M.; Vorholt, J.A. The General Stress Response in Alphaproteobacteria. *Trends Microbiol.* **2015**, *23*, 164–171. [CrossRef]
66. Gourion, B.; Sulser, S.; Frunzke, J.; Francez-Charlot, A.; Stiefel, P.; Pessi, G.; Vorholt, J.A.; Fischer, H.-M. The PhyR-σ^{EcfG} Signalling Cascade Is Involved in Stress Response and Symbiotic Efficiency in *Bradyrhizobium japonicum*. *Mol. Microbiol.* **2009**, *73*, 291–305. [CrossRef]
67. Ledermann, R.; Bartsch, I.; Müller, B.; Wülser, J.; Fischer, H.-M. A Functional General Stress Response of *Bradyrhizobium diazoefficiens* Is Required for Early Stages of Host Plant Infection. *Mol. Plant Microbe Interact.* **2018**, *31*, 537–547. [CrossRef] [PubMed]
68. Bastiat, B.; Sauviac, L.; Bruand, C. Dual Control of *Sinorhizobium meliloti* RpoE2 Sigma Factor Activity by Two PhyR-Type Two-Component Response Regulators. *J. Bacteriol.* **2010**, *192*, 2255–2265. [CrossRef] [PubMed]
69. Sauviac, L.; Philippe, H.; Phok, K.; Bruand, C. An Extracytoplasmic Function Sigma Factor Acts as a General Stress Response Regulator in *Sinorhizobium meliloti*. *J. Bacteriol.* **2007**, *189*, 4204–4216. [CrossRef]
70. Jans, A.; Vercruysse, M.; Gao, S.; Engelen, K.; Lambrichts, I.; Fauvart, M.; Michiels, J. Canonical and Non-Canonical EcfG Sigma Factors Control the General Stress Response in *Rhizobium etli*. *MicrobiologyOpen* **2013**, *2*, 976–987. [CrossRef]
71. Foreman, R.; Fiebig, A.; Crosson, S. The LovK-LovR Two-Component System Is a Regulator of the General Stress Pathway in *Caulobacter crescentus*. *J. Bacteriol.* **2012**, *194*, 3038–3049. [CrossRef]
72. Lang, C.; Barnett, M.J.; Fisher, R.F.; Smith, L.S.; Diodati, M.E.; Long, S.R. Most *Sinorhizobium meliloti* Extracytoplasmic Function Sigma Factors Control Accessory Functions. *mSphere* **2018**, *3*, e00454-18. [CrossRef] [PubMed]
73. Flechard, M.; Fontenelle, C.; Trautwetter, A.; Ermel, G.; Blanco, C. *Sinorhizobium meliloti rpoE2* Is Necessary for H_2O_2 Stress Resistance during the Stationary Growth Phase. *FEMS Microbiol. Lett.* **2009**, *290*, 25–31. [CrossRef] [PubMed]
74. Ledermann, R.; Emmenegger, B.; Couzigou, J.-M.; Zamboni, N.; Kiefer, P.; Vorholt, J.A.; Fischer, H.-M. *Bradyrhizobium diazoefficiens* Requires Chemical Chaperones To Cope with Osmotic Stress during Soybean Infection. *mBio* **2021**, *12*, e00390-21. [CrossRef] [PubMed]
75. Ravcheev, D.A.; Khoroshkin, M.S.; Laikova, O.N.; Tsoy, O.V.; Sernova, N.V.; Petrova, S.A.; Rakhmaninova, A.B.; Novichkov, P.S.; Gelfand, M.S.; Rodionov, D.A. Comparative Genomics and Evolution of Regulons of the LacI-Family Transcription Factors. *Front. Microbiol.* **2014**, *5*, 294. [CrossRef]